

Predictive modelling for solar thermal energy systems: A comparison of support vector regression, random forest, extra trees and regression trees



Muhammad Waseem Ahmad^{*}, Jonathan Reynolds, Yacine Rezgui

BRE Centre for Sustainable Engineering, School of Engineering, Cardiff University, Cardiff, CF24 3AA, United Kingdom

ARTICLE INFO

Article history:

Received 30 April 2018

Received in revised form

17 July 2018

Accepted 19 August 2018

Available online 28 August 2018

Keywords:

Artificial intelligence

Extra trees

Random forest

Decision trees

Ensemble algorithms

Solar thermal energy systems

ABSTRACT

Predictive analytics play an important role in the management of decentralised energy systems. Prediction models of uncontrolled variables (e.g., renewable energy sources generation, building energy consumption) are required to optimally manage electrical and thermal grids, making informed decisions and for fault detection and diagnosis. The paper presents a comprehensive study to compare tree-based ensemble machine learning models (random forest – RF and extra trees – ET), decision trees (DT) and support vector regression (SVR) to predict the useful hourly energy from a solar thermal collector system. The developed models were compared based on their generalisation ability (stability), accuracy and computational cost. It was found that RF and ET have comparable predictive power and are equally applicable for predicting useful solar thermal energy (USTE), with root mean square error (RMSE) values of 6.86 and 7.12 on the testing dataset, respectively. Amongst the studied algorithms, DT is the most computationally efficient method as it requires significantly less training time. However, it is less accurate (RMSE = 8.76) than RF and ET. The training time of SVR was 1287.80 ms, which was approximately three times higher than the ET training time.

© 2018 The Authors. Published by Elsevier Ltd. This is an open access article under the CC BY-NC-ND license (<http://creativecommons.org/licenses/by-nc-nd/4.0/>).

1. Introduction

The existing building sector, which is one of the most substantial consumers of energy, contributes towards 40% of world's total energy consumption and accounts for 30% of the total CO₂ emissions (Ahmad et al., 2016a). Currently, energy systems are predominantly based on fossil fuels. However, to reduce CO₂ emissions and tackle the challenge of mitigating climate change, such systems need to include a combination of fluctuating renewable energy resources (RES) such as wind and solar energy, along with residual resources (e.g., biomass) (Lund et al., 2014). In recent years, more focus is being placed on increasing the energy efficiency, incorporating renewable energy generation sources and optimally managing the fluctuation of energy supply (Mathiesen et al., 2015). Energy generation through direct harnessing of solar radiation is one of the largest renewable energy technologies currently exploited worldwide. Solar energy currently constitutes a significant proportion of

renewable energy generation in the EU. The majority of this energy generation is currently harnessed through solar photovoltaic systems for producing electricity, accounting for around 4.3% of total installed renewable energy in the EU in 2016 (Eurostat, 2016). In contrast, solar thermal energy only accounts for around 2% of installed renewable generation. To ensure a renewable energy future, it is vital that heating and cooling demands are also met by renewable energy technologies. It is expected that solar thermal energy will continue to grow to play a significant future role in this endeavour. Solar thermal energy is most commonly harvested via glazed evacuated tube collectors or flat-plate collectors. In a typical flat-plate collector, solar radiation passes through a transparent cover. A large portion of this energy is absorbed by a blackened absorber surface, which is then transferred to a fluid in tubes (Kalogirou, 2004). Evacuated thermal collectors contain a heat pipe inside a vacuum-sealed tube. The heat pipe is attached to a black copper fin that fills the absorber plate. These collectors also contain a protruded metal tip on top of each tube, which is attached to the sealed pipe. A small amount of fluid, contained in the heat pipe, undergoes an evaporating-condensing cycle. The fluid evaporates and rises to the heat sink region, where it dissipates latent heat, and

^{*} Corresponding author.

E-mail addresses: AhmadM3@cardiff.ac.uk (M.W. Ahmad), reynoldsj8@cardiff.ac.uk (J. Reynolds), rezguiy@cardiff.ac.uk (Y. Rezgui).

condenses back to the collector to repeat the process (Kalogirou, 2004). Solar thermal energy is most commonly harvested on a smaller residential scale. However, solar thermal generation is increasingly being integrated into larger scale projects in combination with supplementary generation as part of wider, district-scale energy systems (Sawin et al., 2017). Prediction models, a core component of smart-grids, of solar thermal systems, could be used for following applications;

- The comparison of predicted performance with the actual performance of a system could be used as an indication of potential failure (e.g. shaded solar thermal collector, valve failure, solar collector fault, etc.). Models can be used to automatically activate an alarm in case of any problem so that any potential malfunction could be corrected promptly.
- Optimal control of decentralised energy systems can be achieved by using prediction models of uncontrolled variables (e.g., energy generation from RES, building heating demand, etc.). It allows building users, owners, mechanical and electrical (M&E) engineers, thermal-grid operators, etc. to make informed decisions such as shifting energy consumption to off-peak periods, increasing penetration of RES, etc.
- Prediction models could be used to analyse performance characteristics of different solar collector types such as flat and evacuated, different system configurations, etc. The models could be used by engineers, while designing a system, to achieve maximum efficiency with minimum cost and computational resources.

1.1. Related work

Prediction and modelling of solar thermal and renewable energy generation systems have been addressed in the existing body of literature. Broadly, two methods are available for modelling solar thermal systems; one is built upon the analytical understanding of the thermodynamic phenomena within the system, the second is a rapidly growing field based on computational intelligence techniques. This section will give an overview of the two methods through reviewing existing studies within the literature as well as outlining the novelty and originality of the present work.

Calculation of the performance of a solar thermal system is highly complex when using an analytical modelling approach. An overview of the theoretical equations governing the thermal dynamics of solar thermal collectors can be found in Duffie and Beckman (2013). Often, computational models are required to capture the physical phenomena at the expense of a large amount of computational time and power. A combination of finite difference and electrical analogy models were used in (Notton et al., 2013; Motte et al., 2013) to calculate the outlet temperature of a building integrated solar thermal collector. The accuracy of the numerical model was validated against experimental data allowing the authors to simulate future geometric and material design alterations to improve the efficiency of the solar collector. A numerical modelling approach was applied to a building integrated, aerogel covered, solar air collector in Dowson et al. (2012). From this, the authors were able to calculate outlet temperatures and collector efficiency from weather conditions. The model outputs were validated to within 5% of the measured values over a short measurement period. As a result, the authors could simulate much longer time periods to demonstrate the potential efficiency and financial payback of their proposed solution. A numerical modelling approach within the MATLAB environment applied to a v-groove solar collector was developed in Karim et al., (2014). The resulting model can predict the air temperature at any part of the

solar collector as well as the efficiency to within a 7% relative error. Whilst the described modelling approaches achieve accurate calculations of solar thermal performance; they do require highly complex mathematical modelling using thermodynamic principles. In these cases, the time and effort are justified due to the experimental nature of the solar collectors presented. However, in general, analytical models are computationally intensive, and in most cases, exhaustive exploration of parametric space for online control is not feasible. Also, most consumers would not require such detailed modelling of solar thermal collector systems. Therefore, simpler and more generic modelling approaches are required to be able to forecast the key variables, namely outlet temperature, and useful heat energy gain.

Data-driven models are often the preferred choice where fast responses are required (e.g., near real-time control applications) and where pertinent information for detailed simulation/numerical models is not available (Ahmad et al., 2016b). Data-driven models capture the underlying physical behaviour by identifying trends in the data and do not require detailed information about system characteristics. These techniques have been extensively applied to model or predict several parameters related to energy systems. For example solar PV generation was predicted in (Kharb et al., 2014; Yap and Karri, 2015; Yona et al., 2007), wind energy in (Cadenas and Rivera, 2009; Catalão et al., 2011; Kusiak et al., 2009) and building energy demand in (Ahmad et al., 2017; Benedetti et al., 2016; Chae et al., 2016). They have proven accuracy and applicability to energy scheduling problems with the significant advantage of simplicity and speed.

Application of machine learning algorithms for solar thermal collectors is so far limited and most of the previous research studies are focused on using artificial neural networks. A recent article by Reynolds et al. (2018) provides an overview of different modelling techniques for solar thermal energy systems. An adaptive neuro-fuzzy inference system (ANFIS) modelling approach was applied to a solar thermal system in (Yaici and Entchev, 2016). The model used time, ambient temperature, solar radiation, and stratification tank temperatures at the previous to predict the heat input from the solar thermal collector and tank temperature at the next timestep. The resulting predictions were compared with an ANN based on the same data and found both models performed comparably. Similarly, Géczy-Víg and Farkas (2010) used an ANN to model the temperature at different layers of a solar-connected stratification tank using temperatures from the previous timestep as an input as well as mass flow rate and solar radiation. The model achieved accurate predictions with an average deviation of 0.2 °C but only predicted 5 minutes ahead. An ANN was used in (Kalogirou et al., 2014) to allow prediction of daily energy gain and resulting thermal storage tank temperature of a large-scale solar thermal systems. Several combinations of input data were trialled including daily solar radiation, average ambient temperature, and storage tank initial conditions. Results on test data achieved an R^2 value of around 0.93 although a total daily figure is less likely to be useful than a daily profile with hourly or sub-hourly resolution. Both (Caner et al., 2011; Esen et al., 2009) applied ANN to calculate the efficiency of experimental solar air collectors. Both of these studies achieved high R^2 values, however, both case studies have a limited amount of training data. Therefore, required many, potentially difficult to monitor, input features. Sözen et al. (2008) also aimed to calculate the efficiency of a solar thermal collector using an ANN. More generic inputs were used such as solar radiation, surface temperature, and tilt angles. The model could accurately predict the efficiency of a solar thermal collector with a maximum deviation of 2.55%. The authors argued that the resulting, more generic, model can therefore be used throughout the region to calculate the efficiency of any similar flat plate collector. Kalogirou et al. (2008)

utilised ANN prediction of solar thermal system temperatures to develop an automatic fault diagnosis module. The ANN models were trained using fault free TRNSYS simulation data. The predictions of fault free temperature resulting from the trained ANN were compared to the real system data from which the likelihood of system failure could be determined. The fault detection system was shown to effectively detect three types of failure relating to the collector, the pipe insulation, and the storage tank. Liu et al. (2015) tested the applicability of two types of ANN, multi-layer feed-forward neural networks (MLFN) and general regression neural networks (GRNN) as well as a support vector machines (SVM) model to calculate the heat collection rate and heat loss coefficient of solar thermal systems. They aimed to allow calculation using simple, portable test instruments rather than the current method which requires deconstruction of the entire system. They find that the MLFN is best suited to predicting the heat collection rate but the GRNN performed better at predicting the heat loss coefficient. Table 1 summarizes previous work on modelling solar thermal energy systems.

1.2. Motivation, objectives and contributions

Thermal performance analyses of the solar thermal system are too complex; analytical models are computationally intensive and require a considerable amount of computational time to accurately model these systems. On the other hand, data-driven approaches

are seldom used and most of the used data-driven approaches are based on artificial neural networks or its variants. To the best of authors' knowledge, there are not any studies that investigated the applicability of tree-based methods and in particular tree-based ensemble methods for modelling solar thermal systems. From the literature, it was also found that some of the most widely used machine learning algorithms (e.g. artificial neural networks, decision trees) are prone to be unreliable due to their instability issues (Breiman et al., 1996). The instability of these algorithms may result in large variations in the model output due to small changes in the input data (Breiman et al., 1996; Wang et al., 2018). As highlighted in the above section, the developed models from this research could be used for real-time optimisation, fault detection and diagnosis. Therefore, instability of models could cause failure of the prediction models as these application rely on the accuracy of the developed models. In the early 1990s, more advanced machine learning techniques, ensemble learning, were developed to overcome these instability issues (Wang et al., 2018; Hansen and Salamon, 1990).

Ensemble-based methods generally perform better than the individual learners that construct them, as they overcome their limitations and there might not be enough data available to train a single model with better generalisation capabilities (Dietterich, 2000; Fan et al., 2014). The paper compares the accuracy in predicting hourly useful solar thermal energy (USTE) by using four different machine learning algorithms: random forest (RF), extremely randomised trees/extra tree (ET), decision trees (DT) and

Table 1
Review summary of solar thermal system modelling techniques.

Ref	Method	Input Parameters	Output Parameters	Model Accuracy	Location
(Notton et al., 2013)	Numerical Modelling	Thermodynamic parameters, weather conditions	Component temperatures	5–10% Relative RMSE	France
(Dowson et al., 2012)	Numerical Modelling	Thermodynamic parameters, weather conditions, inlet temperature	Solar thermal outlet temperature	–	UK
(Karim et al., 2014)	Numerical Modelling	Thermodynamic parameters, weather conditions, inlet conditions	Component temperatures, air temperatures, efficiency	<7% Relative Error	–
(Yaïci and Entchev, 2016)	ANFIS	Ambient temperature, solar radiation, previous tank temperatures	Tank temperature, heat input, solar fraction	1–9% Relative Error	Canada
(Géczy-Víg and Farkas, 2010)	ANN	Ambient temperature, solar radiation, mass flow rate, previous tank temperature	Tank temperature at 8 layers	0.24° Average Error	Hungary
(Kalogirou et al., 2014)	ANN	Average daily temperature, total daily solar radiation, starting tank temperature	Daily energy output, final tank temperature	$r = 95\text{--}96\%$	–
(Caner et al., 2011)	ANN	Date, time, inlet and outlet collector temperature, tank temperature, ambient and surface temperature, solar radiation	Collector efficiency	$R^2 = 0.9967$, RMSE = 1.73%	Turkey
(Esen et al., 2009)	WNN, ANN	Ambient temperature, solar radiation, absorbing plate temperatures	Efficiency, outlet temperature	$R^2 = 0.9992/0.9994$, RMSE = 0.0094/0.0034	Turkey
(Sözen et al., 2008)	ANN	Date, time, surface temperature, solar radiation, declination, azimuth and tilt angles	Efficiency	$R^2 = 0.983$	Turkey
(Kalogirou et al., 2008)	ANN	Global radiation, beam radiation, ambient temperature, incidence angle, wind speed, humidity, flow availability, input temperature	Collector inlet and outlet temperature, storage inlet and outlet temperature	$R^2 = 0.9920, 0.9996$, 0.8823, 0.9504	Cyprus
(Liu et al., 2015)	MLFN, GRNN, SVM	Tube length, number and radius, hot water mass, collector area, tilt angle, final temperature	Heat collection rate, heat loss coefficient	RMSE = 0.14/0.73 (MLFN), = 0.33/0.71 (GRNN), = 0.29/0.73 (SVM)	China

Note - ANFIS (Adaptive Neuro-Fuzzy Inference System), ANN (Artificial Neural Network), WNN (Wavelet Neural Network), MLFN (Multi-Layer Feed-Forward Neural Network), GRNN (General Regression Neural Network), SVM (Support Vector Machine), RMSE (Root Mean Squared Error).

support vector regression (SVR). The work also does not take into account system control variables as input features, which increases the complexity of the problem. Furthermore, the models developed in this study can provide a 24-h ahead prediction of USTE at an hourly time-step rather than the total daily sum or parameters with limited applicability such as efficiency.

The research presented in this paper mainly addresses the following aspects;

- the use of ensemble-based techniques for solar thermal systems as current application of machine learning algorithms are limited and most of the previous research work are focussed on artificial neural networks and its variants,
- the use of tree-based ensemble methods to provide insight into the analysis of the variable importance of each input feature, i.e. using them as feature selection tools. In most of the existing research, domain knowledge is widely used to reduce input variable space. The presented analysis will allow researchers to gain better understanding of the modelled systems, and,
- to demonstrate that tree-based ensemble methods can improve the prediction and stability of the developed model. Also, they are more computationally efficient as compared to the conventional methods used in the literature (for example, support vector regression in our case).

The rest of the paper is organised as follows: Section 2 describes the principles of random forest, extra trees, decision trees and support vector regression. The methodology of the developed prediction models is presented in Section 3, along with feature selection process and results. Prediction results and discussion are detailed in Section 4, whereas concluding remarks and future research directions are presented at the end of the paper.

2. Machine learning methods

Four data-driven algorithms for predicting useful solar thermal energy are introduced in this section. These algorithms include extra trees (ET), random forest, decision trees, and support vector regression (SVR).

2.1. Support vector machines

Support vector machine is one of the most widely used computational intelligence technique applied in building energy and renewable energy generation prediction and modelling applications. It provides a sparse pattern of solutions and flexible control on the model complexity (Deng et al., 2018), making it highly effective in solving non-linear problems even with a small sample of training datasets. SVM adopts the structure risk minimisation (SRM) principle; which instead of only minimising the training error (this the principle of traditional empirical risk minimisation), minimises an upper bound of the generalisation error consisting of the sum of the training error and a confidence interval (Dong et al., 2005). SVM is commonly applied with different kernel functions to map the input space into a higher dimensional feature space, which introduces the non-linearity in the solution, and to perform a linear regression in the feature space (Li et al., 2009; Vapnik, 2013). Assuming normalised input variables consist of a vector X_i , and Y_i is the useful solar thermal energy (i represents the i^{th} data-point in the dataset). In this case, a set of data points can be defined as $\{(X_i, Y_i)\}_{i=1}^N$, where N is the total number of samples. An SVM regression approximates the function using the form given in Equation (1) (Dong et al., 2005; LIN et al., 2006).

$$Y = f(X) = W \cdot \phi(X) + b \tag{1}$$

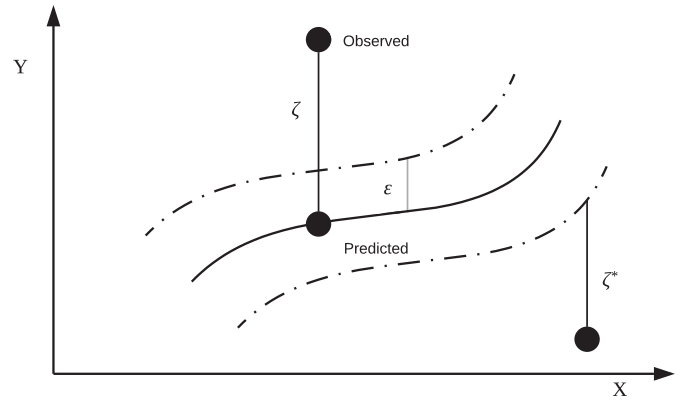


Fig. 1. The parameters of the support vector regression. Source (Dong et al., 2005; Li et al., 2009).

In Equation (1), $\phi(X)$ denotes the high-dimensional space. A regularised risk function, given in Equation (2), is used to estimate coefficients W and b (Li et al., 2009).

$$\text{Minimise} : \frac{1}{2} \|W\|^2 + C \frac{1}{N} \sum_{i=1}^N L_{\epsilon}(Y_i, f(X_i)) \tag{2}$$

$$L_{\epsilon}(Y_i, f(X_i)) = \begin{cases} 0, & |Y_i - f(X_i)| \leq \epsilon \\ |Y_i - f(X_i)| - \epsilon, & \text{others} \end{cases} \tag{3}$$

$\|W\|^2$ is known as regularised term and C is the penalty parameter to determine the flexibility of the model. The second term of Equation (2) is the empirical error and is measured by the ϵ -intensity loss function (Equation (3)). This defines a ϵ tube shown in Fig. 1. If the predicted value is within the tube, then the loss is zero. Whereas if it is outside the tube, then the loss is the magnitude of the difference between the predicted value and the radius ϵ of the tube (Li et al., 2009). To estimate W and b , the above equation is transformed into the primal objective function given by Equation (4) (Li et al., 2009).

$$\text{Minimise} \zeta_1, \zeta_1^*, W, b : \frac{1}{2} \|W\|^2 + C \frac{1}{N} \sum_{i=1}^N (\zeta_i - \zeta_i^*) \tag{4}$$

$$\text{Subject to:} \begin{cases} Y_i - W \cdot \phi(x_i) - b \leq \epsilon + \zeta_1 \\ W \cdot \phi(x_i) + b \leq \epsilon + \zeta_1^*, & i = 1, 2, \dots, N \\ \zeta_1 \geq 0 & \zeta_1^* \geq 0 \end{cases}$$

In the above equations, ζ_1 and ζ_1^* are the slack variables. By introduction of kernel function $k(X_i, X_j)$, Equation (4) is written as below;

$$\text{Minimise} \{\alpha_i\}, \{\alpha_i^*\} : \frac{1}{2} \sum_{i=1}^N \sum_{j=1}^N (\alpha_i - \alpha_i^*) (\alpha_j - \alpha_j^*) \cdot k(X_i, X_j) - \epsilon \sum_{i=1}^N (\alpha_i - \alpha_i^*) + \sum_{i=1}^N Y_i (\alpha_i - \alpha_i^*) \tag{5}$$

$$\text{Subject to:} \begin{cases} \sum_{i=1}^N (\alpha_i - \alpha_i^*) = 0 \\ \alpha_i, \alpha_i^* \in [0, C] \end{cases}$$

In Equation (5) α_i, α_i^* are Lagrange multipliers, i and j are different samples. Therefore, Equation (1) becomes (Li et al., 2009);

$$Y = f(X) = \sum_{i=1}^N (\alpha_i - \alpha_i^*) k(X_i, X_j) + b \quad (6)$$

2.2. Random forest

A random forest (RF) is a tree-based ensemble method and was developed to address the shortcomings of traditional Classification and Regression Tree (CART) method. RF consists of a large number of weak decision tree learners, which are grown in parallel to reduce the bias and variance of the model at the same time (Breiman, 2001). For training a random forest, N bootstrapped sample sets are drawn from the original dataset. Each bootstrapped sample is then used to grow an unpruned regression (or classification) tree. Instead of using all available predictors in this step, only a small and fixed number of randomly sampled K predictor are selected as split candidates. These two steps are then repeated until C such trees are grown, and new data is predicted by aggregating the prediction of the C trees. RF uses bagging to increase the diversity of the trees by growing them from different training datasets, and hence reducing the overall variance of the model (Rodriguez-Galiano et al., 2015). A RF regression predictor can be expressed as;

$$\hat{f}_{RF}^C(\mathbf{x}) = \frac{1}{C} \sum_{i=1}^C T_i(\mathbf{x}) \quad (7)$$

where \mathbf{x} is the vectored input variable, C is the number of trees, and $T_i(\mathbf{x})$ is a single regression tree constructed based on a subset of input variables and the bootstrapped samples. RF can natively perform out-of-bag error estimation in the process of constructing the forest by using the samples that are not selected during the training of the i -th tree in the bagging process. This subset is called out-of-bag, which can compute an unbiased estimation of generalisation error without using an external text data subset (Breiman, 2001). RF also enables assessment of relative importance of input features, which is useful for dimensionality reduction to improve model's performance on high-dimensional datasets (Ahmad et al., 2017). The RF switches one of the input variables while keeping the remaining constant, and measures the mean decrease in model's prediction accuracy, which is then used to assign relative importance score for each input variable (Breiman, 2001). Fig. 2 shows the structure of random forest algorithm.

2.3. Extra trees

Extremely randomised trees (or extra trees) (Geurts et al., 2006) algorithm is a relatively recent machine learning techniques and was developed as an extension of random forest algorithm, and is less likely to overfit a dataset (Geurts et al., 2006). Extra tree (ET) employs the same principle as random forest and uses a random subset of features to train each base estimator (John et al., 2016). However, it randomly selects the best feature along with the corresponding value for splitting the node (John et al., 2016). ET uses the whole training dataset to train each regression tree. On the other hand, RF uses a bootstrap replica to train the model.

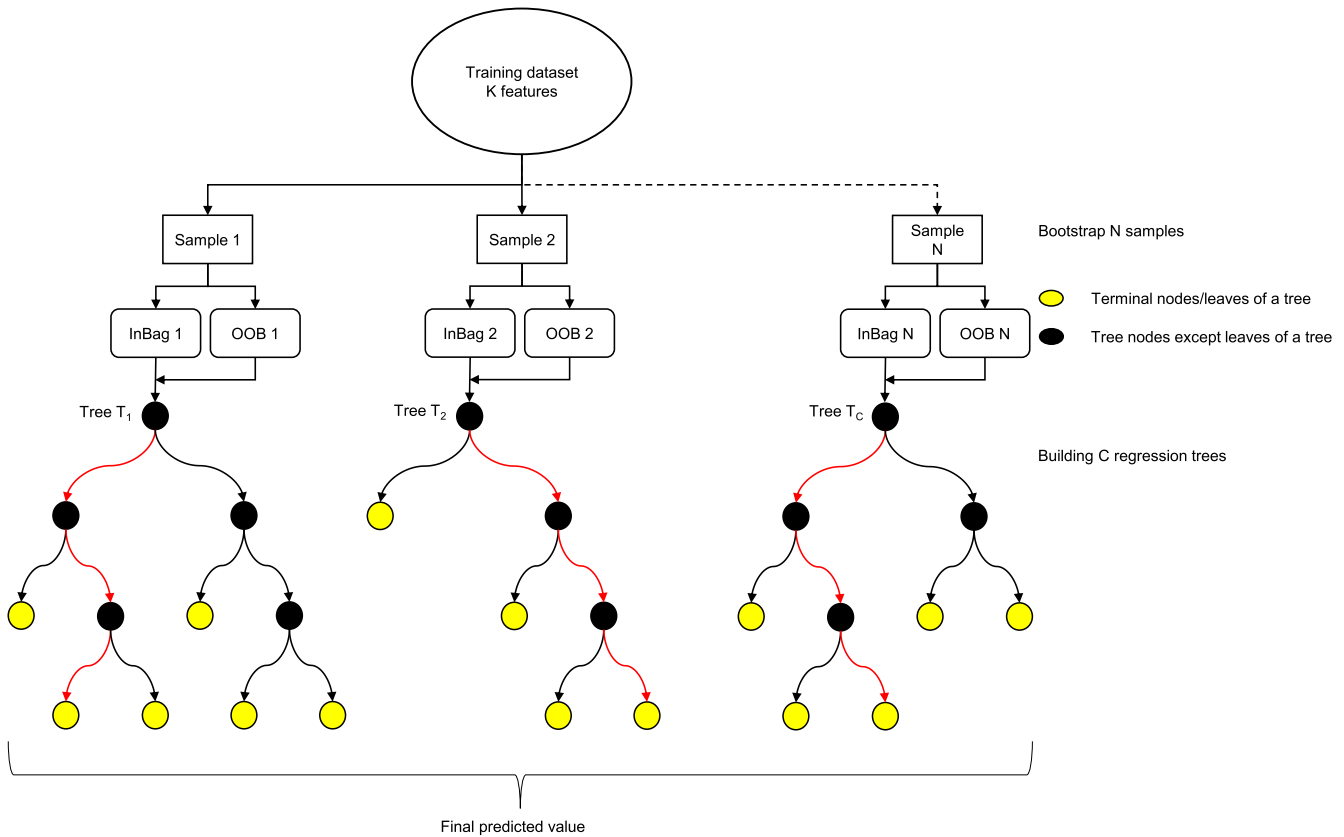


Fig. 2. Structure of random forest.

2.4. Decision trees

A decision tree (DT) is an efficient algorithm for classification and regression problems. The basic idea of the decision tree algorithm is to split a complex problem into several simpler problems, which might lead to a solution that is easier to interpret (Xu et al., 2005). A DT represents a set of conditions, which are hierarchically organised and successively applied from root to leaf of the tree (Breiman et al., 1984). DTs are easy to interpret and their structure is transparent. DTs produce a trained model that can represent logical rules, which can then be used to predict new dataset through the repetitive process of splitting (Ahmad et al., 2017). According to Breiman et al. (1984); in a decision tree method, features of data are referred as predictor variables whereas the class to be mapped is the target variable. For regression problems, the target variables are continuous.

To train a DT model, recursive partitioning and multiple regressions are performed from the training dataset. From the root node of the tree, the data splitting process in each internal node of a rule of the tree is repeated until the stopping criterion is met (Rodriguez-Galiano et al., 2015). In DT algorithm, each leaf node of the tree contains a simple regression model, which only applies to that leaf only. After the induction process, pruning can be applied to improve the generalisation capability of the model by reducing the tree's complexity (Rodriguez-Galiano et al., 2015). For a solar thermal collector application, a simple example of decision tree to predict USTE is depicted in Fig. 3. The output of the decision tree is the useful solar thermal energy. It is worth mentioning that the decision tree is only for demonstration purpose and the actual DT used in the analysis is more complex (i.e., more than two features are considered when looking for best split and the tree is deeper). The decision tree shown in Fig. 3 only considers solar radiation and outdoor dry-bulb air temperature as input variables, and the maximum depth of the tree is restricted to 3.

3. Material and methods

This section details the training and testing datasets, feature selection process and results. The section also details metrics used for assessing models' predictive performance. The implementation of extra trees, random forest, support vector regression included in the scikit-learn (Pedregosa et al., 2011) module of python programming language was used for all developmental and experimental work. The work was carried out on a personal computer (Intel Core i5 2.50 GHz with 16 GB of RAM).

3.1. Data description

The studied solar thermal system is installed at an experimental facility in Chambéry, France and has a total area of 400 m². The solar loop contains a mixture of 60% and 40% water-glycol, and has a density of 1044 kg/m³. The mass flow rate, supply and return temperatures are monitored every minute. The building also has an on-site weather station; which monitors outdoor dry-bulb air temperature, solar radiation, wind speed and direction, relative humidity and atmospheric pressure. In total, after removing outliers and missing values, the training and testing datasets contained 5580 data samples. The data was collected from 01st April 2017 to 25th January 2018. Predicting USTE is a challenging task as none of the system variables (i.e. mass flow rate, supply and return temperature) are considered as input variables. The system variables are not available in advance and therefore are not suitable for future predictions (unless separate models are developed for those variables). Also, USTE did not exhibit any clear pattern as opposed to solar PV prediction (which is almost directly related to solar radiation), as it would also depend on energy load on thermal storage. Training data is taken as 70% of the whole dataset, and remaining data samples were used as testing dataset. Fig. 4 displays the scatter plots for each of the input variables with USTE. It is clear that any

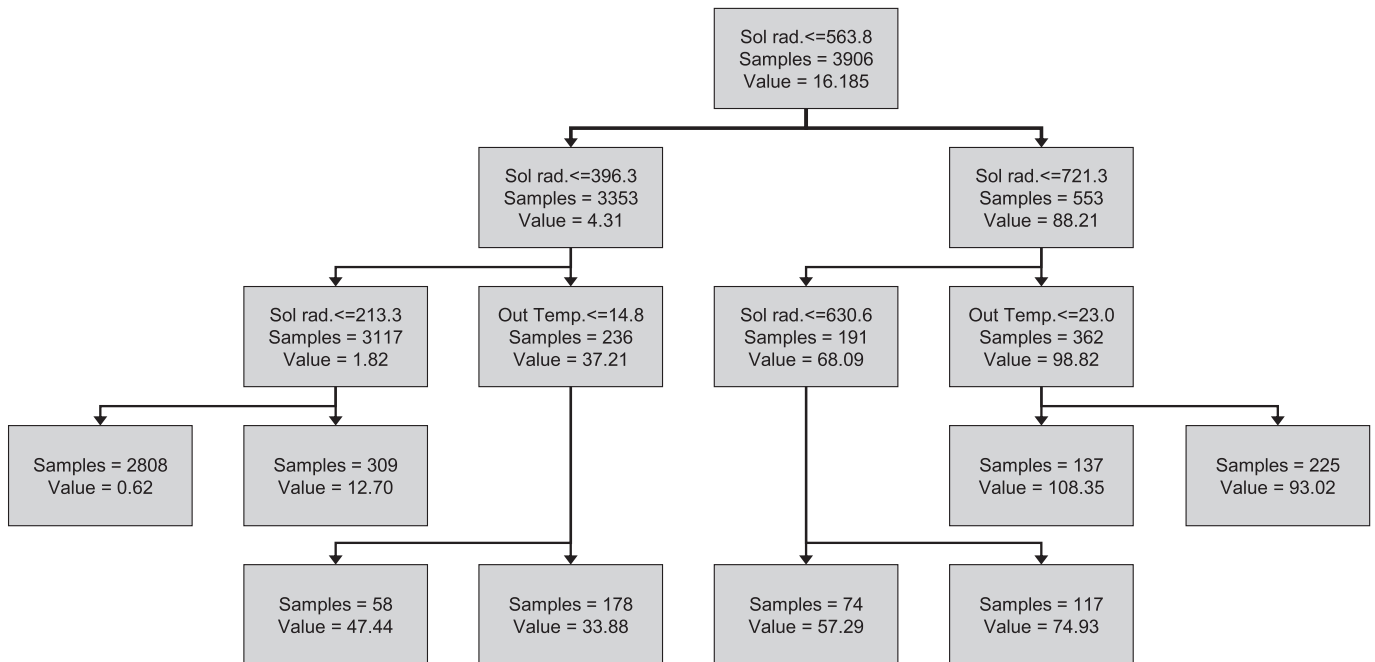


Fig. 3. Decision tree for predicting energy gain from solar collector. Note: Sol rad.: solar radiation, Out Temp.: outdoor dry-bulb air temperature.

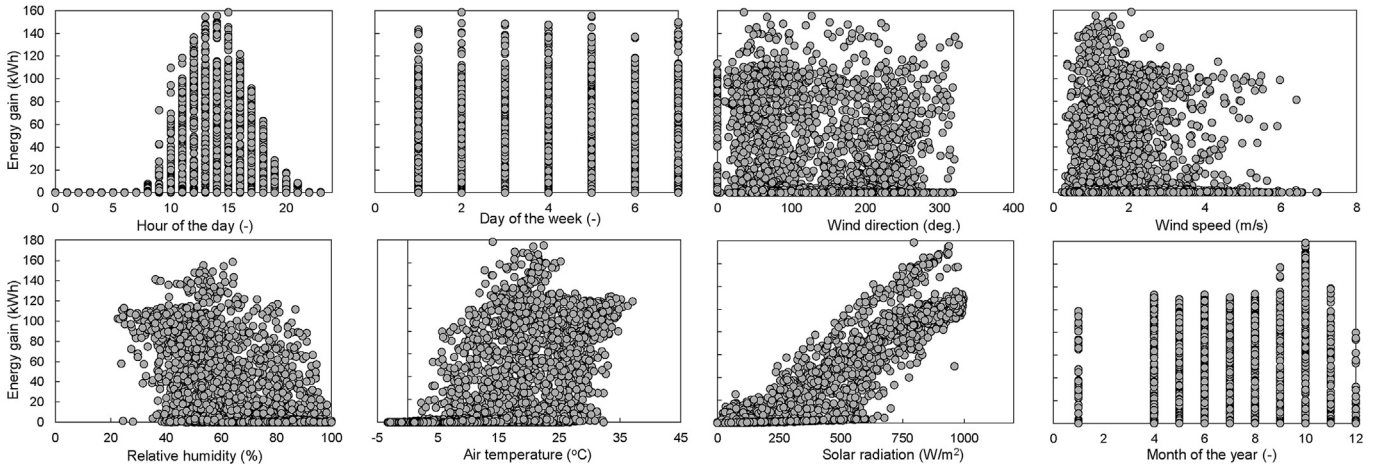


Fig. 4. Scatter plot demonstrating the relation between input and output variables.

relationship of input features and the output variable is not trivial, and simple learners may not be able to accurately predict USTE. It is also important to mention that features were normalised before applying SVR to avoid features in greater numeric ranges dominating those in smaller numeric ranges. In this paper, we will focus on developing machine learning models for useful solar thermal energy (Q_c), without using system controlled and uncontrolled variables (i.e. mass flow rate, and supply and return temperature). The absorption heat transfer rate or USTE, Q_c , can be calculated by using Equation (8) (Karsli, 2007).

$$\dot{Q}_c = \dot{m} \times C_p \times (T_{out} - T_{in}) \quad (8)$$

In Equation (8), \dot{m} is the mass flow rate, C_p is the specific heat of the solar collector fluid, and T_{in} and T_{out} are the inlet and outlet temperatures of the solar collector.

3.2. Uncertainty analysis

To assess the performance of developed models on training and testing datasets; root mean square error (RMSE), mean absolute error (MAE) and the determination coefficient (R^2) were calculated. The determination coefficient was adopted to measure the correlation between the actual and estimated USTE values. The former

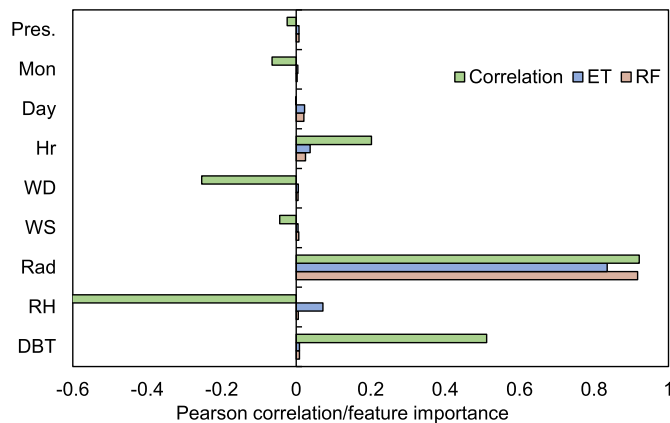


Fig. 5. Feature importance and Pearson correlation for solar thermal useful energy prediction. Notes: Pres.: atmospheric pressure, Mon: month of the year, Day: day of the week, Hr: hour of the day, WD: wind direction, WS: wind speed, Rad: Solar radiation, RH: Outdoor air relative humidity, DBT: outdoor air dry-bulb temperature.

two indicators are defined as below;

$$RMSE = \sqrt{\frac{\sum_{i=1}^N (\mathbf{y}_i - \hat{\mathbf{y}}_i)^2}{N}} \quad (9)$$

$$MAE = \frac{1}{N} \sum_{i=1}^N |\hat{\mathbf{y}}_i - \mathbf{y}_i| \quad (10)$$

where $\hat{\mathbf{y}}_i$ is the predicted value, \mathbf{y}_i is the actual value, and N is the total number of samples. In this work, root mean squared error (RMSE) is used as the primary metric.

3.3. Feature subset selection

Feature selection is an important step in the development of machine learning models. The number of input features may vary from two to hundreds of features, among them many may be unimportant or have lower correlation with the target variables. Previous research works have demonstrated that prediction models are often affected by high variance in the training dataset (Neupane et al., Aung). Feature selection methods increase models' performance on high-dimensional datasets by reducing training time, enhancing model's generalization capability, improving interpretability of the models (Ahmad et al., 2017). Random forest and extra trees also allow the estimation of the importance of each feature in the model. Fig. 5 shows the results of internal calculation carried out by ET and RF algorithms, as well as features' Pearson correlation with hourly useful thermal energy gain. It is interesting to notice that each of the machine learning models has different variable importance score for some of the input features. As an example; for the ET model, outdoor relative humidity has a variable importance score of 0.072. Whereas, RF has a low score for relative humidity (i.e. 0.0058). Solar radiation was considered as the most important feature by both algorithms. As expected, Outdoor dry-bulb air temperature, solar radiation and hour of the day present a positive correlation with the useful solar thermal energy, as demonstrated by their Pearson correlation coefficients. On the other hand, outdoor relative humidity, wind speed, wind direction, the month of the year and atmospheric pressure are negatively related to the useful solar thermal energy. Later in the results, we will discuss that the prediction of USTE could be improved by integrating demand load prediction. The prediction could also be

improved by considering previous hour useful solar thermal energy. However, in the current work, previous hour values are not considered and will need to be investigated in future.

4. Prediction results and discussion

This section details the prediction results obtained with tree-based ensemble machine learning methods (random forest and extra trees), support vector regression and decision trees; which are described in Section 2. This section also details an assessment of the impact of different hyper-parameters on model's performance.

4.1. Hyper-parametric tuning

Model's hyper-parameters has a great influence on its predictive performance, robustness and generalization capability. This section details the selection of optimal hyper-parameters of studied algorithms. For this purpose, a stepwise searching method is used to find optimal values of model's hyper-parameters. In order to prevent over-fitting problems and analyse models' performance on unknown data, a cross-validation approach is used to select optimal hyper-parameters. In *k*-fold cross-validation, the training dataset is divided into *k* subsets of equal size. Each *k* subset is used as a validation dataset, whereas the remaining *k*-1 subsets are used as training dataset. In this study, five-fold validation is performed for selecting optimal hyper-parameters.

4.1.1. Support vector regression

Different factors affect the generalisation capabilities of support vector regression, i.e. to predict unseen data after learning carried out on training dataset. SVR needs the adjustment of (a) kernel function – linear, polynomial, sigmoid and radial-basis (RBF); (b) gamma of the kernel function, except for linear kernel function; (c) degree of the polynomial kernel function; (d) bias on the kernel function, only applicable to the sigmoid and polynomial kernels; (e) penalty parameter (*C*) of the error term and; (f) radius (ϵ). These parameters need to be tuned to make sure that the developed models do not under fit or over fit data.

In the literature, RBF kernel has been widely used for regression problems as it non-linearly maps samples into a high dimensional space, and can easily handle the non-linear relationship between class labels and attributes (Dong et al., 2005). A polynomial kernel function has more hyper-parameters to tune as compared to RBF. Due to its wide use and lower complexity (fewer hyper-parameters to consider), RBF was selected for this study. For RBF, there are three hyper-parameters to tune, i.e., kernel coefficient (γ), penalty parameter of the error term (*C*) and radius (ϵ). According to the definition of the kernel coefficient by Chang and Lin (2011), $\gamma = 1/K$, where *K* is the number of input features. Therefore, for this paper, $\gamma = 1/5$ was used to estimate outlet temperature and useful energy from a solar thermal heating system. Penalty parameter (*C*) of the error term is used to find the trade-off between the model complexity and the degree to which deviations larger than ϵ are tolerated in the optimisation formulation (represented by Equation (4)). A small value of *C* will place a small weight on the training data and therefore will result in an under-fit model. On the contrary, a too large value of *C* will only minimise the empirical risk, and hence will under-fit the training dataset. In this study, a step wise search was used to find optimal values of *C* and ϵ . Initially, ϵ was fixed at 0.1 while varying *C* over the range of 2^{-7} and 2^7 . From results in Fig. 6, it is evident that initially there was significant improvement in the performance of the model with an increase of *C*. However, from the results, it was found that higher values of *C* did not significantly improve the performance and also it was computationally intensive process to train SVR with larger *C* values. Therefore, a value of $C = 2^6$ was selected for further experiments. Too large values of parameter ϵ also deteriorate model's accuracy as it controls the width of the ϵ -intensive zone (Dong et al., 2005). Values of ϵ were varied over the range of 2^{-10} and 2^5 , while keeping $C = 2^6$. It is evident from Fig. 6 that larger values drastically reduce the accuracy of the model. From the results, a value of $\epsilon = 2^{-7}$ was selected as it provided best results.

4.1.2. Random forest, extra trees and decision trees

Tree-based ensemble methods (extra trees and random forest) need the adjustment of three hyper-parameters, i.e. number of trees (*M*), number of minimum samples required for splitting a node (n_{min}) and attribute selection strength parameter (*K*). Parameter *M* represents the total number of trees in the forest and is directly related to the computational cost. Therefore, a reasonable number of trees need to be selected to find a trade-off between predictive power and computational time. For this paper, 100 number of trees were selected in the forest as increasing the number of trees to greater than 100 did not significantly improve prediction results. *K* denotes the number of randomly selected features at each node during the tree growing process, and determines the strength of variable selection process. For most regression problems, this parameter is set to *p*, where *p* is the dimension of input features vector (Geurts et al., 2006).

For ET, DT and RF, it was found that n_{min} did not significantly enhance the performance of the models and therefore a default value of 2 was selected for this parameter. *K* values were varied in the range of (Ahmad et al., 2016a; Kalogirou, 2004) (i.e. total numbers of features selected for model construction process). For ET and DT, *K* = 5 resulted in better results. Whereas, for RF, *K* = 2 produced optimal results. It is worth mentioning that for RF and ET,

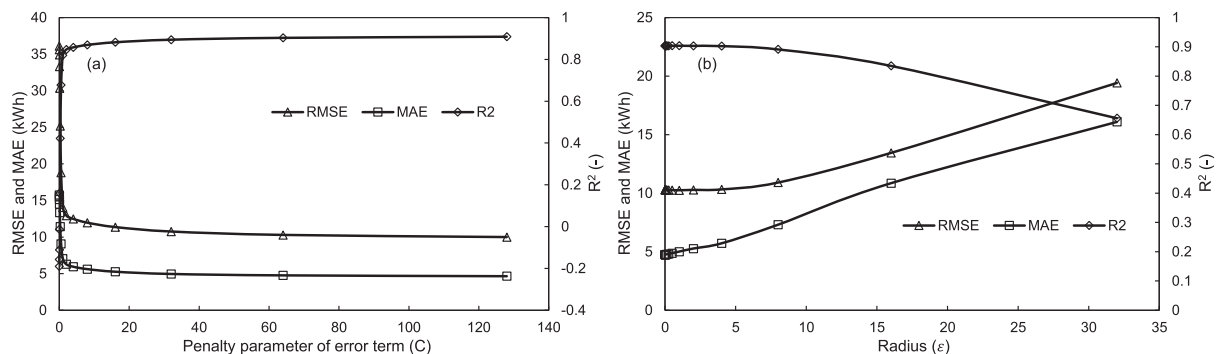


Fig. 6. (a) The results of various *C*, where $\epsilon = 0.1$ and (b) the results of various ϵ , where $C = 2^6$.

Table 2
Results of various d_{\min} for ET, RF and DT.

d_{\min}	Extra trees			Random forest			Decision Tree		
	R^2 (-)	RMSE (kWh)	MAE (kWh)	R^2 (-)	RMSE (kWh)	MAE (kWh)	R^2 (-)	RMSE (kWh)	MAE (kWh)
1	0.7634	16.1055	10.5532	0.5226	22.8774	15.9858	0.7819	15.4619	8.6532
3	0.8944	10.7576	5.1266	0.8982	10.5639	5.9474	0.9081	10.0368	4.5962
5	0.9317	8.6529	3.8446	0.9397	8.1295	4.0182	0.9300	8.7570	3.4668
7	0.9443	7.8122	3.3374	0.9513	7.3028	3.2673	0.9248	9.0782	3.4126
9	0.9523	7.2327	2.9462	0.9552	7.0041	3.0218	0.9239	9.1292	3.3824
10	0.9538	7.1187	2.8737	0.9570	6.8647	2.9168	0.9239	9.1322	3.3420
11	0.9536	7.1287	2.8534	0.9570	6.8660	2.8971	0.9184	9.4566	3.4448
12	0.9537	7.1252	2.8249	0.9560	6.9443	2.9236	0.9201	9.3552	3.3994
13	0.9529	7.1854	2.8382	0.9567	6.8874	2.8882	0.9194	9.3982	3.4511
15	0.9524	7.2227	2.8225	0.9570	6.8680	2.8643	0.9173	9.5232	3.5334
20	0.9526	7.2080	2.8242	0.9553	7.0002	2.8986	0.9099	9.9370	3.6294

Notes— For RF: $n_{\min} = 2, K = 2, M = 100$; for ET: $n_{\min} = 2, K = 5, M = 100$; and for DT: $n_{\min} = 2, K = 5$.

Table 3
Comparison of models on full training and testing datasets.

Model	Training dataset			Testing dataset			Training time (ms)
	R^2 (-)	RMSE (kWh)	MAE (kWh)	R^2 (-)	RMSE (kWh)	MAE (kWh)	
DT	0.957	6.780	2.908	0.930	8.758	3.467	16.00
ET	0.987	3.791	1.630	0.954	7.119	2.874	421.00
SVR	0.917	9.460	4.459	0.903	10.287	4.755	1287.80
RF	0.985	3.955	1.796	0.957	6.8651	2.917	491.60

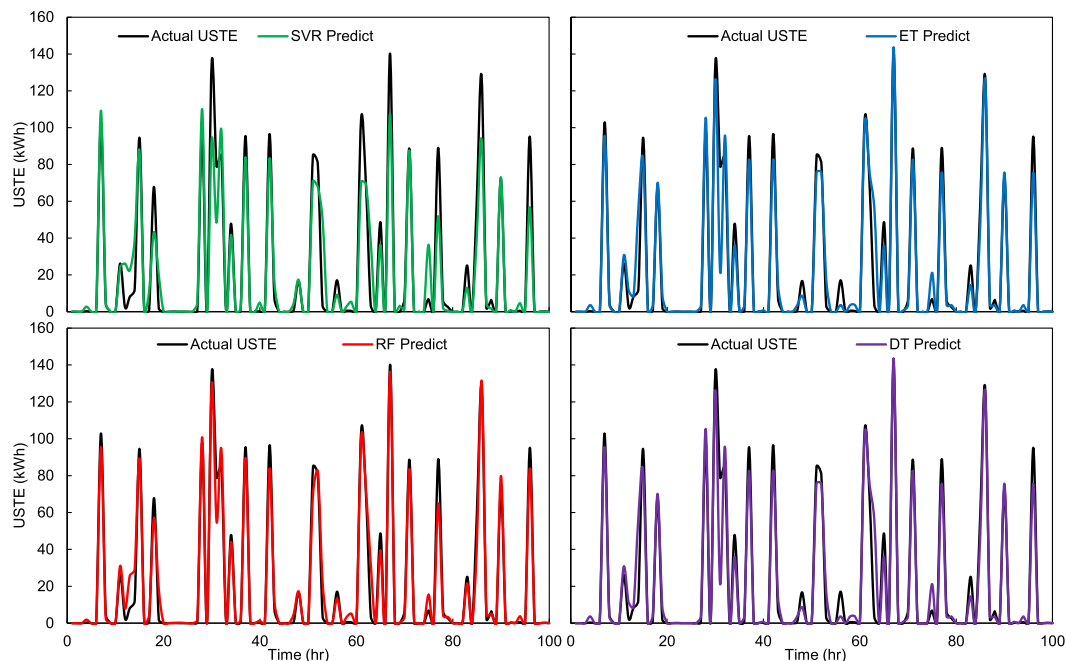


Fig. 7. Prediction results from DT, ET, RF and SVR models on testing data samples.

K parameter did not drastically enhance the results. On the contrary; for DT, K significantly enhance the prediction results, i.e. for values of K equals to 1 and 5, models has R^2 values of 0.8577 and 0.9140, respectively. Table 2 shows the dependence of models' performance on maximum tree depth. Generally, deeper trees resulted in better performance. For ET and RF, trees deeper than 10 started to deteriorate and led to under-fitting. A maximum depth of 5 levels produced marginally better results for DT. From the results, it is evident that for the studied tree-based ensemble algorithms, default parameters are near-optimal and could result in a robust prediction model.

4.2. Model analytical results

Table 3 presents the RMSE, R^2 , and MAE on training and testing datasets for predicting USTE. Generally, errors on the testing dataset show the generalisation capabilities of the developed models. On the other hand, errors on the training dataset show the goodness-of-fit of the developed models. Results in Table 3 suggest that RF and ET achieved the best performance across training and testing datasets. RF achieved RMSE values of 3.96 and 6.86 on training and testing datasets, respectively. Whereas, ET has RMSE values of 3.79 on training and 7.12 on testing datasets. The results

showed that tree-based ensemble methods have nearly comparable performance. SVR has the highest training and testing errors, while DT has achieved marginally better performance as compared to SVR. Fig. 7 illustrates the plot for hourly USTE values predicted by all studied machine learning models vs measured data. It can be concluded that both ET and RF showed strong non-linear mapping generalisation ability, and can be effective in predicting hourly USTE. It was found that best performing methods, RF and ET, over predicted some of the values. Even though the solar radiation values were higher and it was expected to have higher values of USTE. However, the difference between supply and return temperature was small, and therefore the actual value of USTE was lower. In the future work, this problem will need to be tackled, and it is envisaged that considering thermal load on the storage tank as an input variable will further improve models' accuracy. SVR algorithm did not capture the peaks values of USTE and therefore produced worse results as compared to other algorithms. RF closely followed the USTE pattern and therefore performed better on the testing dataset. Also, ET algorithm had the lowest training time (421 ms) than RF (491.60 ms) and SVR (1287.80 ms). Among all studied algorithms, DT was found to be the least computationally intensive. However, this comes at the expense of model's accuracy, as DT has a lower training and testing performances as compared to ET and RF.

4.3. Number of training samples

The number of training samples has two impacts on machine learning algorithms; 1) with the increase in the number of training samples, it is expected that the training time and memory usage during the training phase will increase, and 2) it will increase prediction accuracy of the model. It is worth mentioning here that the training time could also depend on many factors, e.g. the implementation of an algorithm in the programming library, number of input features used, model complexity, feature extraction, input data representation and sparsity (Ahmad et al., 2017). For tree-based ensemble methods, this would also depend on other factors, e.g. number of trees in the forest, maximum depth of a tree, etc. (Ahmad et al., 2017). To demonstrate the sensitivity of machine learning models to the training dataset size and time required to construct a model, different experiments were performed. Fig. 8(a) shows the effect of the number of training data samples on models' predictive performance. Generally, all developed models react in a gradual way to an increase in the training sample size. For all studied algorithms, it was found that increasing the number of samples increases the models' generalisation ability (i.e., increased performance on the unseen testing dataset). It can be seen in Fig. 8

that both RF and ET showed almost same behaviour on training and testing datasets. Their accuracy significantly increased between $n = 100$ and $n = 500$. SVR showed relatively lower accuracy on both training and testing datasets as compared to ET, RF, and DT. It is also important to mention that for tree-based algorithms; the accuracy on training dataset reduced with an increase in the training dataset. For SVR; initially there was a decrease in the accuracy on training dataset, which started to increase after $n = 500$. Fig. 8(b) shows the SVR has significantly higher training time as compared to RF and ET. Please note that DT training time is considerably small and therefore we have not considered it in Fig. 8(b). SVR training time increased exponentially with an increase in the training data samples. ET and RF algorithms have comparable training time on lower number of training samples. However, RF has marginally higher training time for $n > 1500$. In this work, we analysed the impact of number of samples on models' performance and training time. However, in future, training time dependency on algorithm's hyper-parameter will be explored.

5. Conclusions

The paper details the feasibility of using machine learning algorithms to predict hourly useful solar thermal energy. For this purpose, a solar thermal system installed at Chambéry, France was used as a case study. Experiments were performed over the period of April 2017 through January 2018 to gather experimental data for training and testing machine learning models. Different statistical measures were used to appraise the models' prediction performance. The capability of decision tree-based ensemble methods for predicting the USTE has been verified with better accuracy as compared to decision trees and support vector regression. The results also demonstrated that ET and RF algorithms have significantly lower training time, i.e., 421 ms and 491.60 ms, respectively as compared to 1287.80 ms for SVR.

The developed tree-based ensemble methods improved the prediction results and have RMSE values of 6.87 and 7.12 for RF and ET, respectively. Both of these methods were developed to overcome shortcomings of CART, e.g. final tree is not guaranteed to be the optimal tree and generate a stable model. Simple regression trees are not effective for predicting hourly USTE. However, ensembles of these trees have significantly improved models' performance. Tree-based ensemble methods discussed in this paper require fewer tuning parameters and in most cases default hyper-parameters can result in satisfactory performance. The developed models only used weather and time information to predict hourly USTE. To the best of our knowledge, previous works also considered system control variables as inputs to the model. The system

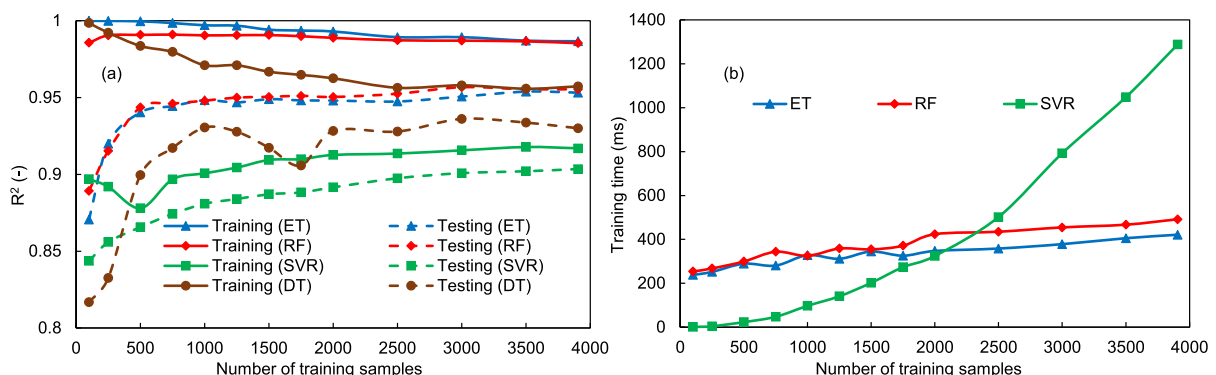


Fig. 8. a) Effect of number of training data samples on prediction accuracy, b) Effect of number of training data samples on training time.

variables are not available in advance and therefore are not suitable for future predictions (unless separate models are developed for these variables). The developed tree-based ensemble methods can achieve accurate and reliable hourly prediction and could be used for fault detection and diagnosis (e.g., solar collector fault, shaded collector area, value fault, etc.), making informed decisions and operational optimisation of multi-vector energy systems. In future work, another promising emerging technique, deep learning, will need to be investigated for solar thermal collectors. Machine learning models for different types of solar collectors and solar collector based systems will need to be developed to cover a wide range of systems. The performance of models will be enhanced in future by incorporating storage load predictions.

Acknowledgement

The work was carried out in the framework of the Horizon 2020 project (Grant reference – 731125) PENTAGON "Unlocking European grid local flexibility through augmented energy conversion capabilities at district-level". The authors acknowledge the financial support from the European Commission. The authors also like to thank Michael Descamps (CEA-INES) for providing valuable experimental data.

Nomenclature

ζ_1, ζ_1^*	slack variables
α_i, α_i^*	Lagrange multipliers
$\ \mathbf{w}\ ^2$	Euclidean norm
$k(X_i, X_j)$	kernel function
ϵ	precision parameter/radius
C	Number of trees/penalty parameter
γ	RBF kernel coefficient
M	number of trees in a forest
x	inputs
N	number of training samples for SVR
C_p	specific heat
T_{out}	outlet temperature of the solar collector

Abbreviations

ANFIS	adaptive neuro-fuzzy inference system
CART	classification and regression trees
ET	extra trees
MAE	mean absolute error
RBF	radial basis function
RF	random forest
SVR	support vector regression
WNN	wavelet neural network
b	bias term
n_{\min}	number of minimum samples required for splitting a tree node
$\emptyset(\mathbf{x})$	non-linear transformation
W	weight vector
T_i	regression tree
\hat{f}_{RF}^C	random forest regression predictor
K	attribute selection parameter
N	number of training samples
y	outputs
\dot{m}	mass flow rate
T_{in}	inlet temperature of the solar collector
ANN	artificial neural network
DT	decision tree
GRNN	general regression neural network
PV	photovoltaic

RES	renewable energy resources
RMSE	root mean square error
USTE	useful solar thermal energy

References

- Ahmad, M.W., Mourshed, M., Mundow, D., Sisinni, M., Rezgui, Y., 2016a. Building energy metering and environmental monitoring – a state-of-the-art review and directions for future research. *Energy Build.* 120 (Suppl. C), 85–102. ISSN 0378-7788, secondoftwo doi: <https://doi.org/10.1016/j.enbuild.2016.03.059>.
- Ahmad, M.W., Mourshed, M., Yuce, B., Rezgui, Y., 2016b. Computational intelligence techniques for HVAC systems: a review. *Building Simulation* 9 (4), 359–398. <https://doi.org/10.1007/s12273-016-0285-4> secondoftwo doi:
- Ahmad, M.W., Mourshed, M., Rezgui, Y., 2017. Trees vs Neurons: comparison between random forest and ANN for high-resolution prediction of building energy consumption. *Energy Build.* 147 (Suppl. C), 77–89. <https://doi.org/10.1016/j.enbuild.2017.04.038>. ISSN 0378-7788, secondoftwo doi:
- Benedetti, M., Cesarotti, V., Introna, V., Serranti, J., 2016. Energy consumption control automation using Artificial Neural Networks and adaptive algorithms: proposal of a new methodology and case study. *Appl. Energy* 165, 60–71. <https://doi.org/10.1016/j.apenergy.2015.12.066> secondoftwo doi:
- Breiman, L., 2001. Random forests. *Mach. Learn.* 45 (1), 5–32.
- Breiman, L., Friedman, J., Stone, C.J., Olshen, R.A., 1984. *Classification and Regression Trees*. CRC press.
- Breiman, L., et al., 1996. Heuristics of instability and stabilization in model selection. *Ann. Stat.* 24 (6), 2350–2383.
- Cadenas, E., Rivera, W., 2009. Short term wind speed forecasting in La Venta, Oaxaca, México, using artificial neural networks. *Renew. Energy* 34 (1), 274–278. <https://doi.org/10.1016/j.renene.2008.03.014> secondoftwo doi:
- Caner, M., Gedik, E., Keçebaş, A., 2011. Investigation on thermal performance calculation of two type solar air collectors using artificial neural network. *Expert Syst. Appl.* 38 (3), 1668–1674. <https://doi.org/10.1016/j.eswa.2010.07.090> secondoftwo doi:
- Catalão, J. P. d. S., Pousinho, H.M.I., Mendes, V.M.F., 2011. Short-term wind power forecasting in Portugal by neural networks and wavelet transform. *Renew. Energy* 36 (4), 1245–1251. <https://doi.org/10.1016/j.renene.2010.09.016> secondoftwo doi:
- Chae, Y.T., Horeh, R., Hwang, Y., Lee, Y.M., 2016. Artificial neural network model for forecasting sub-hourly electricity usage in commercial buildings. *Energy Build.* 111, 184–194. <https://doi.org/10.1016/j.enbuild.2015.11.045> secondoftwo doi:
- Chang, C.-C., Lin, C.-J., 2011. LIBSVM: a library for support vector machines. *ACM Trans. Intell. Syst. Technol. (TIST)* 2 (3), 27.
- Deng, H., Fannon, D., Eckelman, M.J., 2018. Predictive modeling for US commercial building energy use: a comparison of existing statistical and machine learning algorithms using CBECS microdata. *Energy Build.* 163, 34–43. <https://doi.org/10.1016/j.enbuild.2017.12.031>. ISSN 0378-7788, secondoftwo doi:
- Dietterich, T.G., 2000. Ensemble methods in machine learning. In: *International Workshop on Multiple Classifier Systems*, vols. 1–15. Springer.
- Dong, B., Cao, C., Lee, S.E., 2005. Applying support vector machines to predict building energy consumption in tropical region. *Energy Build.* 37 (5), 545–553. <https://doi.org/10.1016/j.enbuild.2004.09.009>. ISSN 0378-7788, secondoftwo doi:
- Dowson, M., Pegg, I., Harrison, D., Dehouche, Z., 2012. Predicted and in situ performance of a solar air collector incorporating a translucent granular aerogel cover. *Energy Build.* 49, 173–187. <https://doi.org/10.1016/j.enbuild.2012.02.007> secondoftwo doi:
- Duffie, J.A., Beckman, W.A., 2013. *Solar Engineering of Thermal Processes*. John Wiley & Sons.
- Esen, H., Ozgen, F., Esen, M., Sengur, A., 2009. Artificial neural network and wavelet neural network approaches for modelling of a solar air heater. *Expert Syst. Appl.* 36 (8), 11240–11248. <https://doi.org/10.1016/j.eswa.2009.02.073> secondoftwo doi:
- Eurostat, 2016. Primary Production of Renewable Energy by Type. URL: <http://ec.europa.eu/eurostat/web/energy/data/main-tables>.
- Fan, C., Xiao, F., Wang, S., 2014. Development of prediction models for next-day building energy consumption and peak power demand using data mining techniques. *Appl. Energy* 127, 1–10. <https://doi.org/10.1016/j.apenergy.2014.04.016> secondoftwo doi:
- Géczy-Vig, P., Farkas, I., 2010. Neural network modelling of thermal stratification in a solar DHW storage. *Sol. Energy* 84 (5), 801–806. <https://doi.org/10.1016/j.solener.2010.02.003> secondoftwo doi:
- Geurts, P., Ernst, D., Wehenkel, L., 2006. Extremely randomized trees. *Mach. Learn.* 63 (1), 3–42. <https://doi.org/10.1007/s10994-006-6226-1> secondoftwo doi:
- Hansen, L.K., Salamon, P., 1990. Neural network ensembles. *IEEE Trans. Pattern Anal. Mach. Intell.* 12 (10), 993–1001. <https://doi.org/10.1109/34.58871> secondoftwo doi:
- John, V., Liu, Z., Guo, C., Mita, S., Kidono, K., 2016. Real-time Lane Estimation Using Deep Features and Extra Trees Regression. Springer International Publishing, Cham, pp. 721–733. https://doi.org/10.1007/978-3-319-29451-3_57 secondoftwo doi:
- Kalogirou, S.A., 2004. Solar thermal collectors and applications. *Prog. Energy Combust. Sci.* 30 (3), 231–295. ISSN 0360-1285, secondoftwo doi: <https://doi.org/10.1016/j.peccs.2004.02.001>.

- Kalogirou, S., Lalot, S., Florides, G., Desmet, B., 2008. Development of a neural network-based fault diagnostic system for solar thermal applications. *Sol. Energy* 82 (2), 164–172. <https://doi.org/10.1016/j.solener.2007.06.010> secondoftwo doi:
- Kalogirou, S., Mathioulakis, E., Belessiotis, V., 2014. Artificial neural networks for the performance prediction of large solar systems. *Renew. Energy* 63, 90–97. <https://doi.org/10.1016/j.renene.2013.08.049> secondoftwo doi:
- Karim, M., Perez, E., Amin, Z.M., 2014. Mathematical modelling of counter flow v-groove solar air collector. *Renew. Energy* 67, 192–201. <https://doi.org/10.1016/j.renene.2013.11.027> secondoftwo doi:
- Karsli, S., 2007. Performance analysis of new-design solar air collectors for drying applications. *Renew. Energy* 32 (10), 1645–1660. <https://doi.org/10.1016/j.renene.2006.08.005>. ISSN 0960-1481, secondoftwo doi:
- Kharb, R.K., Shimi, S., Chatterji, S., Ansari, M.F., 2014. Modeling of solar PV module and maximum power point tracking using ANFIS. *Renew. Sustain. Energy Rev.* 33, 602–612. <https://doi.org/10.1016/j.rser.2014.02.014> secondoftwo doi:
- Kusiak, A., Zheng, H., Song, Z., 2009. Short-term prediction of wind farm power: a data mining approach. *IEEE Trans. Energy Convers.* 24 (1), 125–136. <https://doi.org/10.1109/TEC.2008.2006552> secondoftwo doi:
- Li, Q., Meng, Q., Cai, J., Yoshino, H., Mochida, A., 2009. Applying support vector machine to predict hourly cooling load in the building. *Appl. Energy* 86 (10), 2249–2256. <https://doi.org/10.1016/j.apenergy.2008.11.035>. ISSN 0306-2619, secondoftwo doi:
- LIN, J.-Y., CHENG, C.-T., CHAU, K.-W., 2006. Using support vector machines for long-term discharge prediction. *Hydrol. Sci. J.* 51 (4), 599–612. <https://doi.org/10.1623/hysj.51.4.599> secondoftwo doi:
- Liu, Z., Li, H., Zhang, X., Jin, G., Cheng, K., 2015. Novel method for measuring the heat collection rate and heat loss coefficient of water-in-glass evacuated tube solar water heaters based on artificial neural networks and support vector machine. *Energies* 8 (8), 8814–8834. <https://doi.org/10.3390/en8088814> secondoftwo doi:
- Lund, H., Werner, S., Wiltshire, R., Svendsen, S., Thorsen, J.E., Hvelplund, F., Mathiesen, B.V., 2014. 4th Generation District Heating (4GDH): integrating smart thermal grids into future sustainable energy systems. *Energy* 68, 1–11. <https://doi.org/10.1016/j.energy.2014.02.089>. ISSN 0360-5442, secondoftwo doi:
- Mathiesen, B.V., Lund, H., Connolly, D., Wenzel, H., Østergaard, P.A., Möller, B., Nielsen, S., Ridjan, I., Karnøe, P., Sperling, K., Hvelplund, F.K., 2015. Smart Energy Systems for coherent 100% renewable energy and transport solutions. *Appl. Energy* 145, 139–154. ISSN 0306-2619, secondoftwo doi: <https://doi.org/10.1016/j.apenergy.2015.01.075>.
- Motte, F., Notton, G., Cristofari, C., Canaletti, J.-L., 2013. A building integrated solar collector: performances characterization and first stage of numerical calculation. *Renew. Energy* 49, 1–5. <https://doi.org/10.1016/j.renene.2012.04.049> secondoftwo doi:
- B. Neupane, W. L. Woon, Z. Aung, Ensemble prediction model with expert selection for electricity price forecasting, *Energies* 10 (1).
- Notton, G., Motte, F., Cristofari, C., Canaletti, J.-L., 2013. New patented solar thermal concept for high building integration: test and modeling. *Energy Procedia* 42, 43–52. <https://doi.org/10.1016/j.egypro.2013.11.004> secondoftwo doi:
- Pedregosa, F., Varoquaux, G., Gramfort, A., Michel, V., Thirion, B., Grisel, O., Blondel, M., Prettenhofer, P., Weiss, R., Dubourg, V., et al., 2011. Scikit-learn: machine learning in Python. *J. Mach. Learn. Res.* 12 (Oct), 2825–2830.
- Reynolds, J., Ahmad, M.W., Rezgui, Y., 2018. Holistic modelling techniques for the operational optimisation of multi-vector energy systems. *Energy Build.* 169, 397–416. <https://doi.org/10.1016/j.enbuild.2018.03.065>. ISSN 0378-7788, secondoftwo doi:
- Rodriguez-Galiano, V., Sanchez-Castillo, M., Chica-Olmo, M., Chica-Rivas, M., 2015. Machine learning predictive models for mineral prospectivity: an evaluation of neural networks, random forest, regression trees and support vector machines. *Ore Geol. Rev.* 71 (804 – 818) <https://doi.org/10.1016/j.oregeorev.2015.01.001>. ISSN 0169-1368, secondoftwo doi:
- J. L. Sawin, F. Sverrisson, K. Seyboth, R. Adib, H. E. Murdock, C. Lins, I. Edwards, M. Hullin, L. H. Nguyen, S. S. Prillianto, et al., reportRenewables 2017 Global Status Report .
- Sözen, A., Menlik, T., Ünvar, S., 2008. Determination of efficiency of flat-plate solar collectors using neural network approach. *Expert Syst. Appl.* 35 (4), 1533–1539. <https://doi.org/10.1016/j.eswa.2007.08.080> secondoftwo doi:
- Vapnik, V., 2013. *The Nature of Statistical Learning Theory*. Springer Science & Business Media.
- Wang, Z., Wang, Y., Zeng, R., Srinivasan, R.S., Ahrentzen, S., 2018. Random Forest based hourly building energy prediction. *Energy Build.* 171, 11–25. <https://doi.org/10.1016/j.enbuild.2018.04.008>. ISSN 0378-7788, secondoftwo doi:
- Xu, M., Watanachaturaporn, P., Varshney, P.K., Arora, M.K., 2005. Decision tree regression for soft classification of remote sensing data. *Rem. Sens. Environ.* 97 (3), 322–336. <https://doi.org/10.1016/j.rse.2005.05.008>. ISSN 0034-4257, secondoftwo doi:
- Yaïci, W., Entchev, E., 2016. Adaptive Neuro-Fuzzy Inference System modelling for performance prediction of solar thermal energy system. *Renew. Energy* 86, 302–315. <https://doi.org/10.1016/j.renene.2015.08.028> secondoftwo doi:
- Yap, W.K., Karri, V., 2015. An off-grid hybrid PV/diesel model as a planning and design tool, incorporating dynamic and ANN modelling techniques. *Renew. Energy* 78, 42–50. <https://doi.org/10.1016/j.renene.2014.12.065> secondoftwo doi:
- Yona, A., Senjyu, T., Saber, A.Y., Funabashi, T., Sekine, H., Kim, C.-H., 2007. Application of neural network to one-day-ahead 24 hours generating power forecasting for photovoltaic system. In: *International Conference on Intelligent Systems Applications to Power Systems*, 2007. ISAP 2007, vols. 1–6. IEEE (r).